



# Inkjet-printed Ag grid combined with Ag nanowires to form a transparent hybrid electrode for organic electronics



Tao Ye<sup>a</sup>, Li Jun<sup>a</sup>, Li Kun<sup>a,c</sup>, Wang Hu<sup>a,c</sup>, Chen Ping<sup>a</sup>, Duan Ya-Hui<sup>a</sup>, Chen Zheng<sup>a</sup>, Liu Yun-Fei<sup>a,b</sup>, Wang Hao-Ran<sup>a</sup>, Duan Yu<sup>a,\*</sup>

<sup>a</sup> State Key Laboratory on Integrated Optoelectronics, College of Electronic Science and Engineering, Jilin University, Jilin, 130012, China

<sup>b</sup> Computer Science and Technology Department, Jilin University, Jilin, 130012, China

<sup>c</sup> College of Science, Changchun University of Science and Technology, Changchun, 130012, China

## ARTICLE INFO

### Article history:

Received 26 August 2016

Received in revised form

30 October 2016

Accepted 30 October 2016

Available online 9 November 2016

### Keywords:

Transparent conductive electrode

Flexible substrate

Inkjet-printed Ag nanowire

Ag grid

Organic light-emitting diodes

## ABSTRACT

Networks of silver nanowires (AgNW) have been shown to facilitate high transparency, high conductivity, and good mechanical stability. However, the loose characteristic and local insulation problems due to gaps between the nanowires limit their application as electrodes. This study investigates an inkjet-printed Ag grid combined with AgNW to form a transparent hybrid electrode. The printed Ag grid on AgNW film connects the gaps between the Ag nanowires to increase the overall electric conductivity. The printed Ag-grid/AgNW hybrid electrodes have low resistivity ( $22.5 \Omega/\square$ ) while maintaining a high transmittance (87.5%). These values are similar to standard indium tin oxide (ITO) on glass which has resistivity of  $20 \Omega/\square$  and transmittance of 89% at 550 nm. In addition, these hybrid electrodes are also very flexible when fabricated on a photopolymer substrate. A spin-coating process combined with a peel-off process enable the fabrication of flexible ultra-smooth Ag-grid/AgNW electrodes. We tested the transparent and flexible electrode as the anode of a flexible organic light emitting diode (F-OLED). The light emitting layer of the F-OLED is 35 nm thick tris-(8-hydroxyquinoline) aluminum doped with 0.5% 10-(2-benzothiazolyl)-2,3,6,7-tetrahydro-1,1,7,7-tetramethyl-1H,5H,11H-(1)-benzopyrroprano(6,7-8-Ij) quinolizin-11-one. The maximum brightness and current efficiency of the F-OLED are  $10000 \text{ cd/m}^2$  and  $12 \text{ cd/A}$ , respectively, even when bent around a radius of 2 mm. The good performance of the device with Ag-grid/AgNW hybrid electrodes show that enhanced conductive inkjet-printed Ag nanoparticles combined with Ag nanowires can produce high quality electrodes for flexible organic optoelectronic devices.

© 2016 Elsevier B.V. All rights reserved.

## 1. Introduction

Transparent conductive electrodes (TCEs) play an important role in the fabrication and development of organic optoelectronic devices, such as organic light emitting diodes (OLEDs) [1]. The added attribute of flexibility creates the prospect of producing wearable electronic devices [2,3]. High optical transmittance and low resistivity, however, are the key properties of TCEs. Much research has been conducted to find suitable materials; candidate materials include metal nanowires [4,5], metal-grids [6,7], conductive polymers [8,9], carbon nanotubes [10,11] and graphene [12,13]. Metal nanowires are often considered as the most promising materials to

replace indium tin oxide (ITO) in flexible optoelectronic devices because of their excellent electrical, optical, and mechanical properties. In particular, silver nanowires (AgNW) have attracted significant attention, with several reported applications as electrodes in flexible OLEDs (F-OLEDs) [14,15]. However, AgNW electrodes still need to overcome two critical problems: I. The AgNW deposited on bare substrates tends to be very rough. The high surface roughness of metal nanowire sheets, consisting of multiple metal nanowires stacked in irregular mesh structures, frequently cause short-circuit problems when thin active layers are coated on the sheets [16]; II. AgNW can be removed easily due to their poor adhesion or friction. In our earlier work, we reported that a peel-off process with a flexible polymer substrate is a good way to solve both of these problems [17]. However, the loose characteristic and unwanted insulation due to gaps within the random AgNW network limit their application as electrode materials [18].

\* Corresponding author.

E-mail address: [duanyu@jlu.edu.cn](mailto:duanyu@jlu.edu.cn) (D. Yu).

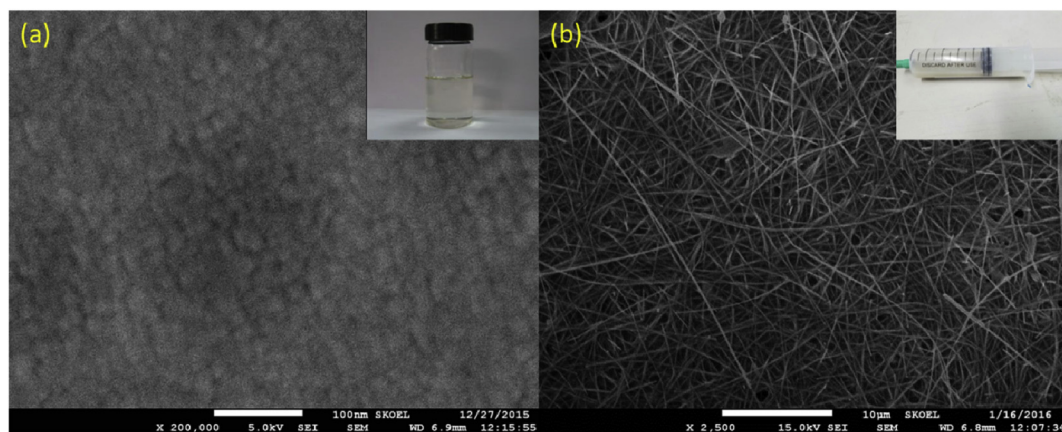


**Fig. 1.** SEM images of Ag nanoparticles and AgNW. (a) Ag nanoparticles spin-coated on Si (inset) showing the Kunshan Hisense Inkjet-605C silver ink. (b) AgNW on Si (inset) showing the BlueNano Company AgNW.

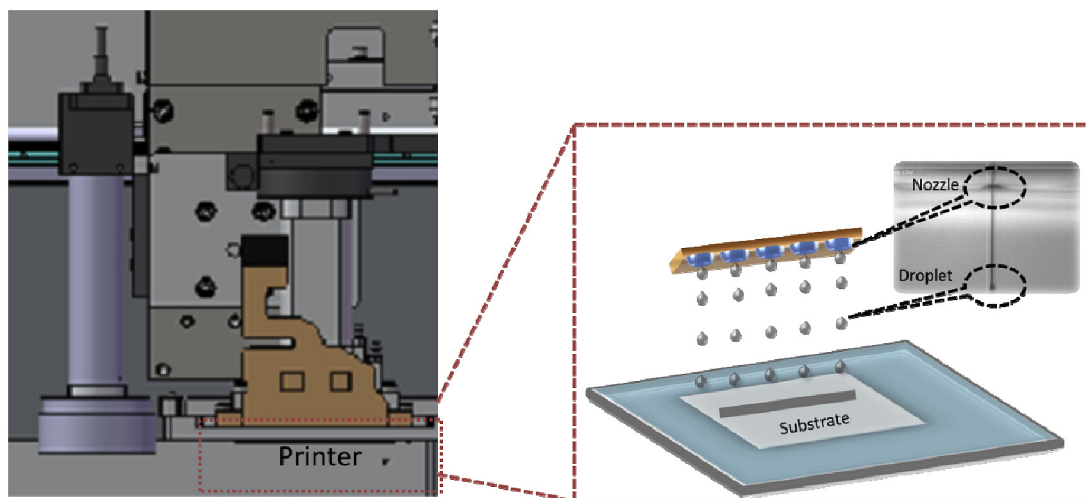


**Fig. 2.** Schematic of the ink printing process using the IJDAS-T300 inkjet printer.

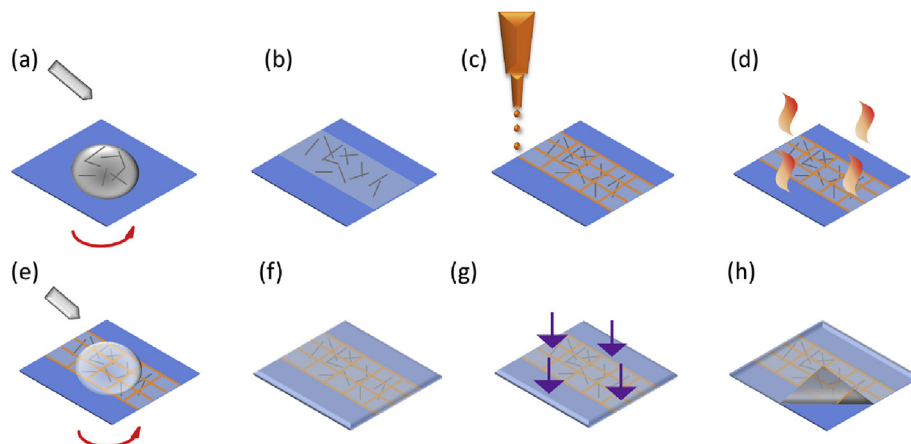
A significantly improved network of AgNW may enable TCEs with metallic grid structures that retain a high conductivity while permitting near 100% optical transmission through “holes” in the grid [19]. Some studies were conducted on the fabrication of metal grid electrodes using e-beam [20] or photolithography [21]. Most of the fabrication methods use vacuum processes or require precise mask alignment steps, which are too time consuming for cost effective commercial use. Inkjet printing has attracted much attention for the production of TCEs because it is a potentially simple and fast process, mask-less, non-contact, and produces little material waste [22,23]. Both AgNW and metal-grid-based transparent electrodes are promising candidates for TCEs. However, metal-grid/AgNW hybrid TCEs, prepared via inkjet printing, have not yet been investigated.

In this paper, we investigate the fabrication of Ag-grid/AgNW hybrid transparent conducting electrodes using inkjet printing and spin-coating. By inserting an inkjet-printed Ag grid on top of the AgNW electrodes, the high sheet resistance of the spin-coated AgNW electrodes can be reduced. We find that the Ag grid on AgNW film is capable of bridging the gaps within the Ag nanowires and thereby increases the electric conductivity. The Ag grid can also connect the loose Ag nanowires, reinforce its connectivity, and increase its mechanical stability. This allows the AgNW to be peeled

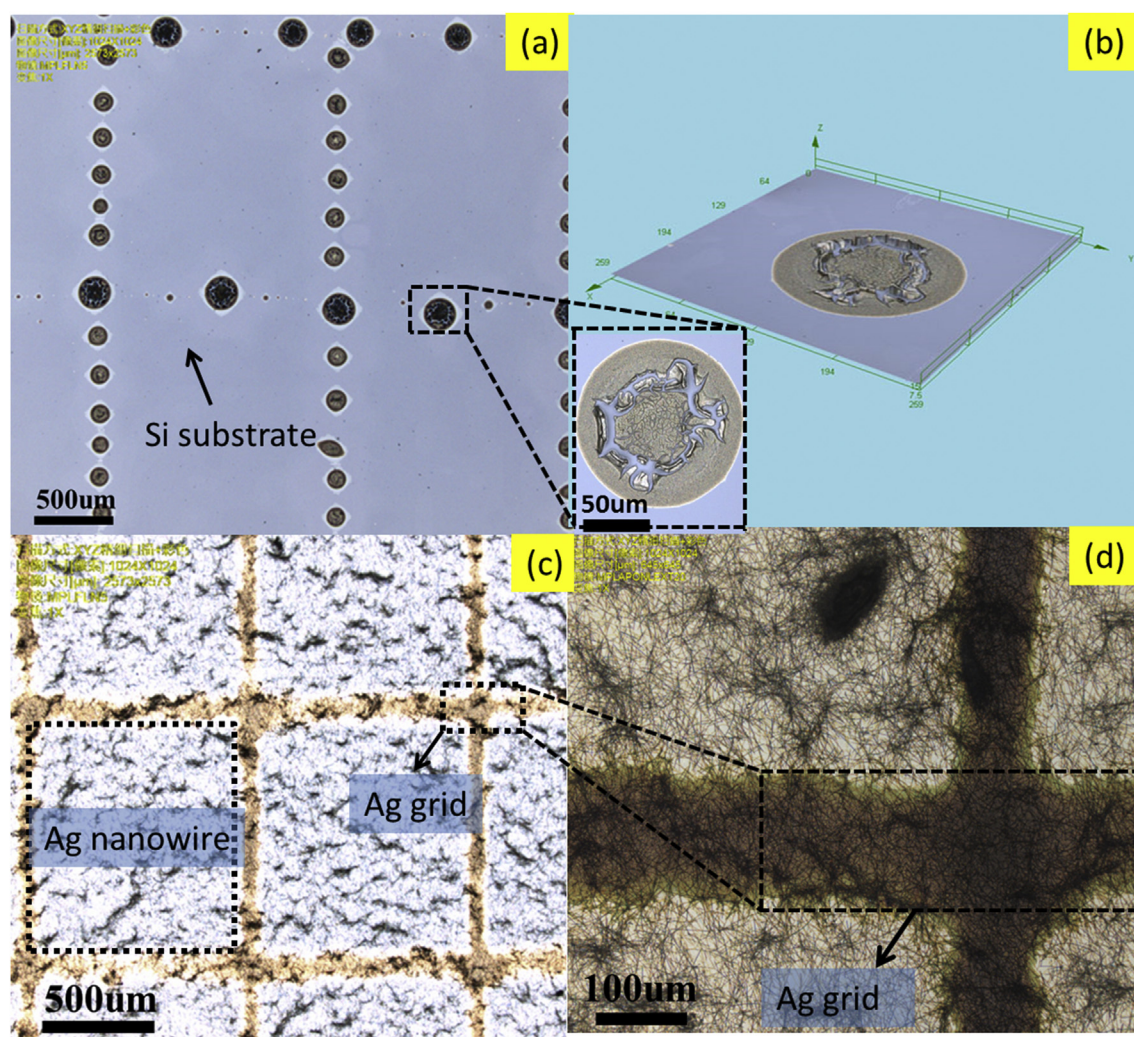
off the silicon wafer completely and to produce a hybrid electrode with an ultra-smooth surface. For the printed Ag-grid/AgNW hybrid electrodes, we measured a low resistivity of  $22.5\Omega/\square$ , and a high transmittance of 87.5%. This approach was successfully used to manufacture the electrodes for F-OLEDs. The resulting devices exhibit a brightness and efficiency comparable with commercial ITO electrodes on glass. In addition, the F-OLEDs made with this method also have excellent flexibility and are mechanically robust.

## 2. Experimental details

The AgNW was obtained from BlueNano (Cornelius, NC, USA) [24] with average dimensions of  $90\text{ nm} \times 20\text{ }\mu\text{m}$ , see Fig. 1 (a). We diluted the AgNW solution concentration down to 5 mg/ml. The AgNW solution concentration of 5 mg/ml is the result of our attempt to maximize the electrical and optical properties based on our previous work. We were shaking the suspended AgNW for 10 min to obtain a uniform dispersion, and spin-coated them onto a pre-cleaned Si substrate for 30 s at 8000 rpm. Then, the AgNW dried at room temperature in the ambient environment to evaporate any residual solvent and form a homogeneous, conductive submicron film of AgNW. The Ag grid was then inkjet-printed with Ag-ink from Kunshan Hisense Electronics with an average particle

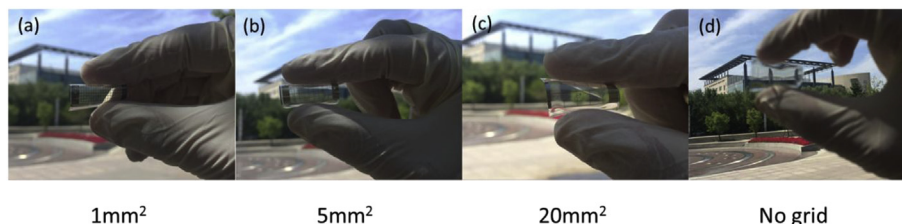


**Fig. 3.** The fabrication processes of the hybrid electrode on a photopolymer substrate. (a). AgNW suspension drop on Si substrate, spin-coating with 8000 rpm/30 s; (b). drying in ambient environment at room temperature; (c). Ag-ink inkjet printed on the AgNW film; (d). annealing at 150°C/10 min; (e). NOA63 drop and spin-coating first at 400 rpm 15s, followed by spinning at 850 rpm/15s; (f). after spin-coating; (g). UV curing at 300 W (370 nm)/4 min; (h). peel-off process.



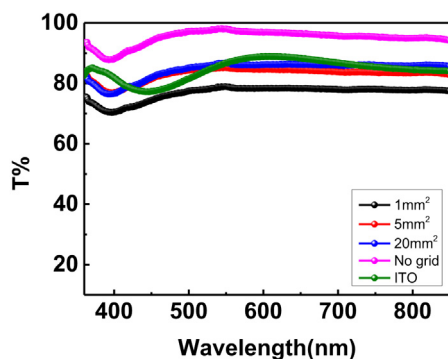
**Fig. 4.** (a). State formation of Ag ink directly inkjet printed on the Si substrate. (b). Enlarged three-dimensional view and inserted plan view. (c). State formation of Ag ink directly inkjet printed on spin-coated AgNW on Si. (d). Enlarged view of Ag grid intersections on spin-coated AgNW on Si; we can see that the Ag nanoparticles are able to fill the gaps between the Ag nanowires. (OLYMPUS).





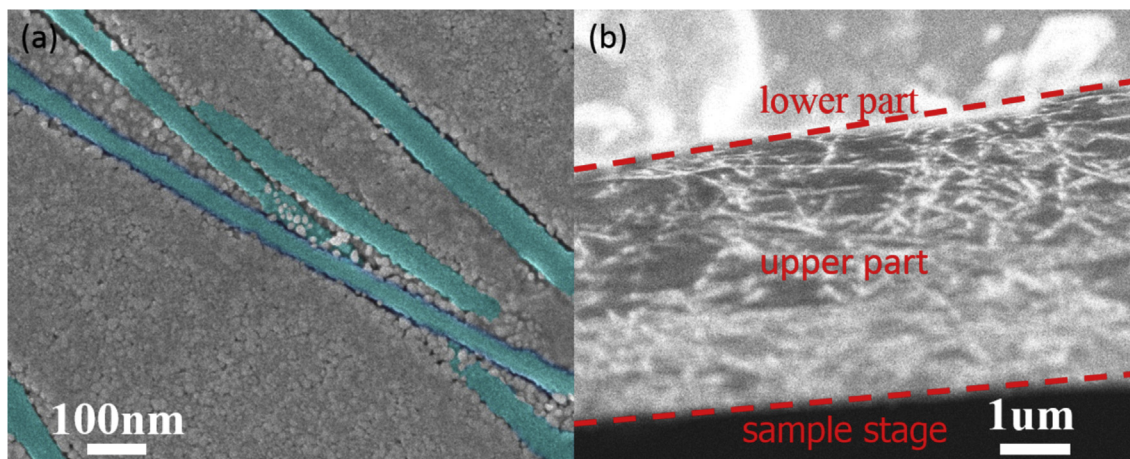
**Fig. 5.** Inkjet-printed Ag-grid/AgNW hybrid electrode. Panel (a) is the area of the Ag grid (1 mm<sup>2</sup>). Panel (b) is the area of the Ag grid (5 mm<sup>2</sup>). Panel (c) is the area of the Ag grid (20 mm<sup>2</sup>). Panel (d) is the electrode without Ag grid.

size of 20 nm [25]. It was synthesized by dissolving 10 wt% Ag nanoparticles in ethanol and another adjustable stabilizer, see Fig. 1 (b). It has a viscosity (7–10 Centipoise) that is suitable for inkjet printing. The surface tension of the used Ag ink is 29 dyne/cm. The inkjet-printing machine is IJDAS300 (Kunshan Hisense Electronics) – see Fig. 2. The process of inkjet-printing involves the ejection of a fixed quantity of ink from a nozzle onto the substrate. The ink uses a sudden, quasi-adiabatic reduction of the chamber volume by a piezoelectric to accomplish this action. In this study, the nozzle of the inkjet printing machine was made of a stainless steel with a diameter of 20  $\mu\text{m}$  – see Fig. 3 (b). First, we injected Ag ink into the cartridge and optimized the pressure manually, based on observation. After setting the print origin, we conducted a



**Fig. 6.** Light transmittance values for several different grid areas of the Ag grid and ITO. (Note: 1 mm<sup>2</sup>: high density inkjet-printed Ag grid; No grid: AgNW without inkjet-printed Ag grid).

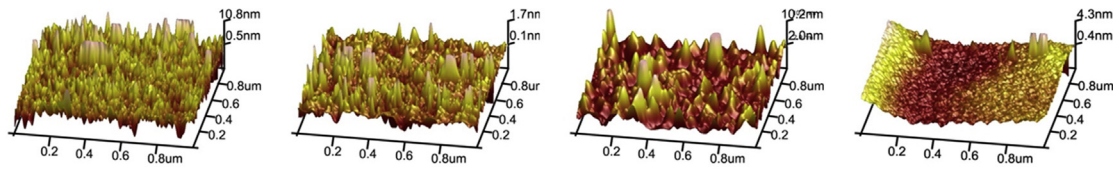
comprehensive printing test. Finally, we printed our default pattern to create the desired Ag grid. During the printing process, we observed the Ag ink output when printing directly on the cleaned Si substrate, see Fig. 4 (a, b). We then spin-coated AgNW on the Si substrate, see Fig. 4 (c, d). It was found that the droplets printed on the cleaned Si substrate are discontinuous. In addition, there is a gap between each set of two droplets, see Fig. 4 (a). However, the droplets printed on spin-coated AgNW on the Si substrate are continuous, see Fig. 4 (c). It can be seen that the Ag nanoparticles are able to fill the gaps between the Ag nanowires. Fig. 4 (b) shows a three-dimensional view and the inserted plan-view of a single silver droplet. The sintering of the Ag ink-droplet produced a coffee-ring effect, the Ag nanoparticles accumulated near the edge of the drops, which was observed using the 3D depth mode of a laser microscope (OLYMPUS). Then, the Ag grid was annealed at 150 °C in an oven. The role of the Ag grid is to bridge the space between the Ag nanowires. NOA63 (Norland Optics, Norland Products, Cranbury, NJ, USA) [26] was then spin coated in two steps. The first step lasts 15 s at 400 rpm, while the second step lasts 15 s at 850 rpm. Then the top of the AgNW film is cast using a photopolymer film, followed by an ultraviolet light treatment (370 nm, 300 W, 240 s). Finally, we pried the edge of the cured photopolymer film from the Si substrate using forceps to peel off the Ag-grid/AgNW and NOA63 from the Si substrate. This film is easily removed because the Ag-grid/AgNW was firmly embedded in the photopolymer film. The Ag grid can also connect the loose silver nanowires and improve its connectivity during the peeling process. As shown in Fig. 5. A high transparent flexible Ag-grid/AgNW electrode was the result of this procedure. Finally, the optical and electronic characteristics of F-OLEDs with Ag-grid/AgNW electrodes as anodes were investigated. The F-OLED structure was as



**Fig. 7.** (a) Top surface SEM image of the inkjet-printed Ag grid on spin coated AgNW after being transferred and embedded in the photopolymer substrate via the spin-coating and peel-off process; (b) cross-section images of the Ag grid/AgNW after being transferred and embedded into the photopolymer substrate by spin-coating and peel-off process.

**Table 1**

Surface morphology of the different areas of Ag-grid/AgNW hybrid electrodes. The Ag-grid/AgNW hybrid electrode with the area of 5 mm<sup>2</sup> even reaches 0.41 nm RMS, which is much smoother than that of AgNW on Si. (Note: no grid: AgNW without inkjet-printed Ag grid).

AFM	1mm <sup>2</sup>	5mm <sup>2</sup>	20mm <sup>2</sup>	No grid
RMS(nm)	1.31	0.415	1.42	0.87
3D image				

follows: a 2 nm MoO<sub>3</sub> buffer layer, 30 nm thick 4,4',4''-Tris(N-3-methylphenyl-N-phenylamino) triphenylamine (m-MTDATA) as the hole injection layer, 20 nm thick NPB as hole transport layer, 35 nm tris-(8-hydroxyquinoline) aluminum (Alq<sub>3</sub>) doped with 0.5% 10-(2-benzothiazolyl)-2,3,6,7-tetrahydro-1,1,7,7-tetramethyl-1H,5H,11H-(1)-benzopyrroprano(6,7-8-I,j)quinolizin-11-one(C545T) as the green light emitting layer, 20 nm thick Alq<sub>3</sub> as electron transport layer, and 0.5 nm thick LiF capped with a 100 nm thick Al as cathode. The active area of the flexible device was 10 × 10 mm. An Agilent B2902A source meter and a Minolta luminance meter LS-110 were used simultaneously to measure the current-density, voltage, and luminance characteristics (J–V–L) of the flexible devices made in air. The electroluminescence (EL) spectra were measured with a Spectroscan PR655 spectrometer at room temperature.

### 3. Results and discussion

In Fig. 6, we compared the light transmittance of different Ag-grid/AgNW flexible conductive films with ITO electrodes on glass. We found that the transmittance of the Ag-grid/AgNW is nearly the same as for ITO. Visible large fluctuations near the UV region were observed from the transmittance of the ITO films. It was also found that control of the Ag grid separation distance is key to determine the transmittance of the hybrid electrodes. The transmittance for the 1 mm<sup>2</sup>, 5 mm<sup>2</sup>, 20 mm<sup>2</sup>, and no grid (AgNW without the printed Ag grid) was slightly lower than for the ITO electrode.

Fig. 7 shows the top surface and cross-section images of the Ag-grid/AgNW after being transferred and embedded into the photopolymer substrate via spin-coating and the peeling process. Fig. 7 (a) shows the AgNW, densely populated and evenly scattered in the photopolymer. The colloidal photopolymer was spin-coated on the Ag-grid/AgNW hybrid thin-film, and the empty spaces in the Ag-grid/AgNW network were filled with photopolymer particles. The photopolymer was cross-linked during UV exposure and the solid–liquid transformation process. Through this process, the Ag-grid/AgNW hybrid thin-film was embedded into the photopolymer.

The cross section of the Ag-grid/AgNW hybrid thin-film is shown in Fig. 7 (b). It shows the top surface of the Ag grid, which was printed on the AgNW. The Ag nanoparticles fill the gaps between the Ag nanowires, and the AgNW was partially wrapped by the Ag nanoparticles. Using this process, the electric conductivity of Ag nanowire layers could be improved by filling the gaps with Ag nanoparticles. The AgNW embedded well in the photopolymer, and the obtained film was quite smooth in contrast to the observed branching on the Si substrate [27]. An electrode could be made using this method without causing damage to the active layer. Moreover, it also reduced physical damage like scratches and detachment, when the AgNW was directly coated on the substrate [28].

The surface morphology of the Ag-grid/AgNW is shown in Table 1. As shown in the table, we can see that the root mean square (RMS) roughness of the Ag-grid/AgNW hybrid thin-film was very

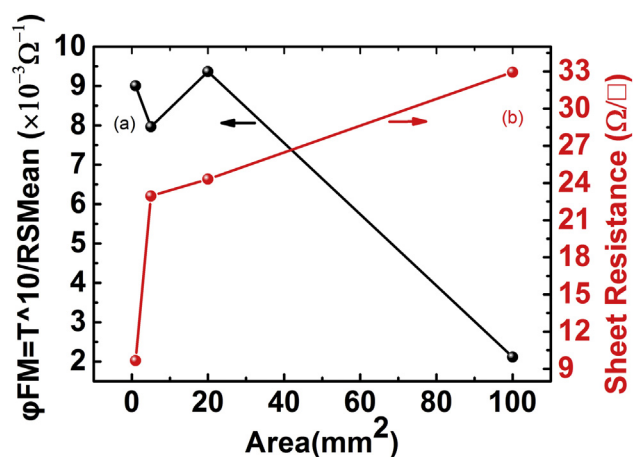


**Fig. 8.** Curve (a) FOM values of the hybrid Ag-grid/AgNW electrode as a function of area. Curve (b) Sheet resistance of the hybrid Ag-grid/AgNW electrode as a function of the Ag-grid surrounded area of AgNW.

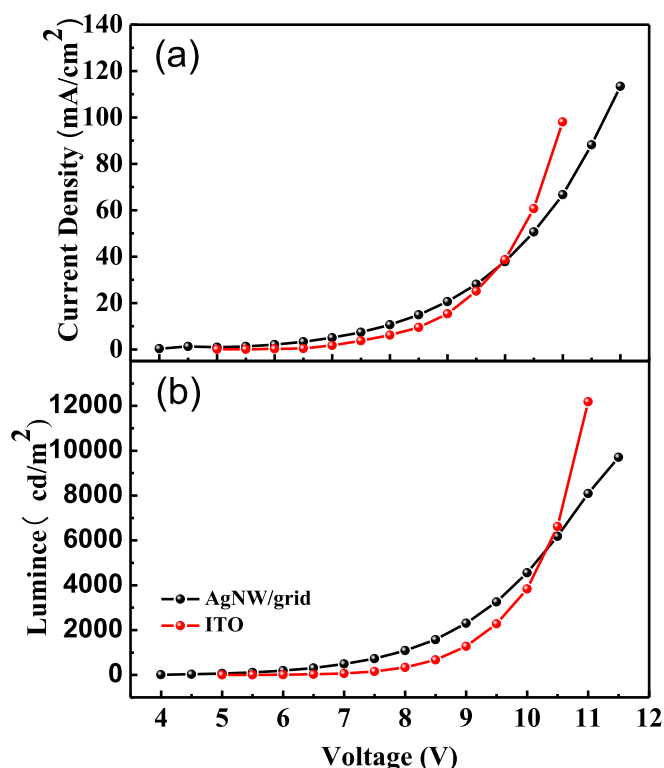


**Fig. 9.** Performance of the bottom-emitting F-OLED with the Ag-grid/AgNW hybrid as transparent anode, with an ITO-OLED of the same structure as reference. Panel (a) shows the current-density/voltage characteristics of the FOLED with 20 mm<sup>2</sup> area Ag-grid/AgNW hybrid electrode and ITO as the reference. Panel (b) shows the luminance as a function of voltage for both devices.

low. It reached 0.41 nm, which is much smoother than the AgNW on Si (RMS = 69.5 nm). This is because the Ag-grid/AgNW thin-film flexible electrode was obtained using a peel-off process and the surface roughness depends on the Si surface (RMS = 0.29 nm) [29]. Our Ag-grid/AgNW hybrid thin-film was flat enough to contact the OLED stack. A decrease in carrier injection and the generation of defects could be avoided because of the smoothness of the Ag-grid/AgNW.

The conductivity of the Ag-grid/AgNW hybrid electrode was also investigated. A four-probe ST-21 system (Kaivo Optoelectronic Technology Co., Ltd) was used to test the resistance of the

electrodes. We can see that the resistance of the electrode increases with increasing Ag-grid separation distance — see Fig. 8 (a). To obtain the optimized Ag grid, the FOM ( $T^{10}/R_{sh}$ ) value, as defined by Haacke, was determined [30]. We calculated the FOM values based on the sheet resistance ( $R_{sh}$ ) and transmittance ( $T$ ) of the Ag-grid/AgNW hybrid electrode — see Fig. 8 (b). When the area of the Ag grid is 20 mm<sup>2</sup> the FOM reaches its maximum. This suggests that the conductivity of the Ag-grid/AgNW hybrid electrode and the Ag grid do not directly correlate with each other.

We also fabricated a bottom-emitting F-OLED with the Ag-grid/AgNW hybrid as transparent anode. The 20 mm<sup>2</sup> Ag grid film and the AgNW with a concentration of 5 mg/ml was compared with an OLED made on ITO. Fig. 9(a) shows that the Ag-grid/AgNW based OLED has a similar current density as the ITO-based OLED. This indicates that our Ag-grid/AgNW hybrid electrode has a hole-injection characteristic that is comparable to ITO. The Ag-grid/AgNW hybrid electrode device also shows similar brightness as the ITO-based OLED — see Fig. 9 (b). However, the luminance of the Ag-grid/AgNW hybrid electrode device is lower than ITO-based OLED after 10.5V, this is because the coverage factor is low, the local current density on the nanowire must be much higher than that in the ITO-based OLED. This would be disadvantage in the hybrid electrode-based OLED regarding local heating and the roll-off [14]. This factor is also the reason of that silver nanowire electrode compared to the ITO electrode still exist some gaps. In fact, it is a trade-off between the silver nanowire coverage factor and local current density. In this work, the value of coverage factor of nanowires is nearly 20%. The maximum current efficiency of the OLED is 11.3 cd/A with high mechanical flexibility, even when bent with a curvature of 2 mm. This value is still very good when compared with ITO based OLEDs, which is 13.5 cd/A at 10 V. Fig. 10 (a) shows the photographs of the devices when bending with a curvature of 2 mm. This clearly demonstrates that the Ag-grid/AgNW hybrid electrode is suitable as TCE in flexible organic electronics thanks to the excellent electrical, optical, and mechanical properties.

#### 4. Conclusions

In summary, we fabricated a flexible bottom-emitting device with inkjet-printed Ag-grid/AgNW hybrid electrodes. The printed Ag-grid line successfully reduced the sheet resistance of the AgNW film. Through optimization of the printed mesh density, and the concentration of the AgNW solution, an electrode with a resistance of 22.5  $\Omega/\square$ , high transparency (87.5%), and relatively high

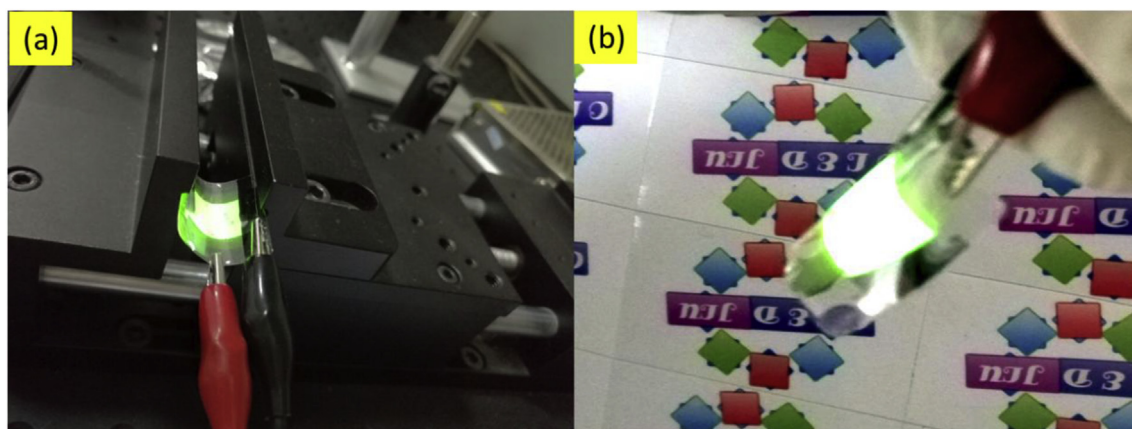


**Fig. 10.** Photographs of the device made with the Ag-grid/AgNW hybrid as transparent anode. Panel (a) shows a photograph of the mechanical bending test with a radius of curvature of 2 mm. Panel (b) shows the device operating at 6 V when bent.



flexibility, could be fabricated. Our results indicate that the AgNW electrode, with its improved properties when combined with an Ag grid, has the potential to provide highly transparent electrodes for eco-friendly, flexible organic optoelectronics of the future.

## Acknowledgements

This study was supported by the International Science & Technology Cooperation Program of China (2014DFG12390), the National High Technology Research and Development Program of China (Grant No. 2011AA03A110), National key research program of China (Grant No. 2016YFB0401001), the National Natural Science Foundation of China (Grant Nos. 61675088, 61275024, 61377026, 61274002, and 61275033), the Scientific and Technological Developing Scheme of Jilin Province (Grant No. 20140101204JC, 20130206020GX, 20140520071JH, 20130102009JC), the Scientific and Technological Developing Scheme of Changchun (Grant No. 13GH02), and the Opened Fund of the State Key Laboratory on Integrated Optoelectronics No. IOSKL2012KF01.

## References

- [1] X. Jiang, F.L. Wong, M.K. Fung, S.T. Lee, Aluminum-doped zinc oxide films as transparent conductive electrode for organic light-emitting devices, *Appl. Phys. Lett.* 83 (2003) 1875–1877.
- [2] W. Wang, M. Song, T.-S. Bae, Y.H. Park, Y.-C. Kang, S.-G. Lee, S.-Y. Kim, D.H. Kim, S. Lee, G. Min, G.-H. Lee, J.-W. Kang, J. Yun, Transparent ultrathin oxygen-doped silver electrodes for flexible organic solar cells, *Adv. Funct. Mater.* 24 (2014) 1551–1561.
- [3] J. Li, S. Qi, J. Liang, L. Li, Y. Xiong, W. Hu, Q. Pei, Synthesizing a healable stretchable transparent conductor, *ACS Appl. Mater. Interfaces* 7 (2015) 14140–14149.
- [4] F. Xu, Y. Zhu, Highly conductive and stretchable silver nanowire conductors, *Adv. Mater.* 24 (2012) 5117–5122.
- [5] H. Lee, M. Kim, I. Kim, H. Lee, Flexible and stretchable optoelectronic devices using silver nanowires and graphene, *Adv. Mater.* 28 (2016) 4541–4548.
- [6] J.A. Jeong, H.K. Kim, J. Kim, Invisible Ag grid embedded with ITO nanoparticle layer as a transparent hybrid electrode, *Sol. Energy Mater. Sol. Cells* 125 (2014) 113–119.
- [7] C.H. Song, C.J. Han, B.K. Ju, J.W. Kim, Photoenhanced patterning of metal nanowire networks for fabrication of ultraflexible transparent devices, *ACS Appl. Mater. Interfaces* 8 (2016) 480–489.
- [8] X. Fan, B. Xu, S. Liu, C. Cui, J. Wang, F. Yan, Transfer-printed PEDOT: PSS electrodes using mild acids for high conductivity and improved stability with application to flexible organic solar cells, *ACS Appl. Mater. Interfaces* 8 (2016) 14029–14036.
- [9] Y. Jin, L. Li, Y. Cheng, L. Kong, Q. Pei, F. Xiao, Cohesively enhanced conductivity and adhesion of flexible silver nanowire networks by biocompatible polymer sol-gel transition, *Adv. Funct. Mater.* 25 (2015) 1581–1587.
- [10] R.H. Baughman, A.A. Zakhidov, W.A. de Heer, Carbon nanotubes – the route toward applications, *Science* 297 (2002) 787–792.
- [11] B. Kim, M.L. Geier, M.C. Hersam, A. Dodabalapur, Inkjet printed circuits on flexible and rigid substrates based on ambipolar carbon nanotubes with high operational stability, *ACS Appl. Mater. Interfaces* 7 (2015) 27654–27660.
- [12] D. Dodoo-Arhin, R.C.T. Howe, G. Hu, Y. Zhang, P. Hiralal, A. Bello, G. Amarutunga, T. Hasan, Inkjet-printed graphene electrodes for dye-sensitized solar cells, *Carbon* 105 (2016) 33–41.
- [13] W. Li, F. Li, H. Li, M. Su, M. Gao, Y. Li, D. Su, X. Zhang, Y. Song, Flexible circuits and soft actuators by printing assembly of graphene, *ACS Appl. Mater. Interfaces* 8 (2016) 12369–12376.
- [14] D. Chen, J. Liang, C. Liu, G. Saldanha, F. Zhao, K. Tong, J. Liu, Q. Pei, Thermally stable silver nanowire-polyimide transparent electrode based on atomic layer deposition of zinc oxide on silver nanowires, *Adv. Funct. Mater.* 25 (2015) 7512–7520.
- [15] S. Kang, T. Kim, S. Cho, Y. Lee, A. Choe, B. Walker, S.J. Ko, J.Y. Kim, H. Ko, Capillary printing of highly aligned silver nanowire transparent electrodes for high-performance optoelectronic devices, *Nano Lett.* 15 (2015) 7933–7942.
- [16] D.S. Ghosh, T.L. Chen, V. Mkhitarian, V. Pruneri, Ultrathin transparent conductive polyimide foil embedding silver nanowires, *ACS Appl. Mater. Interfaces* 6 (2014) 20943–20948.
- [17] Y.-H. Duan, Y. Duan, X. Wang, D. Yang, Y.-Q. Yang, P. Chen, F.-B. Sun, K.-W. Xue, Y. Zhao, Highly flexible peeled-off silver nanowire transparent anode using in organic light-emitting devices, *Appl. Surf. Sci.* 351 (2015) 445–450.
- [18] Y.H. Duan, Y. Duan, P. Chen, Y. Tao, Y.Q. Yang, Y. Zhao, High-performance flexible Ag nanowire electrode with low-temperature atomic-layer-deposition fabrication of conductive-bridging ZnO film, *Nanoscale Res. Lett.* 10 (2015) 90.
- [19] C.E. Hendriks, P.J. Smith, J. Perelaer, A.M.J. Van den Berg, U.S. Schubert, Invisible silver tracks produced by combining hot-embossing and inkjet printing, *Adv. Funct. Mater.* 18 (2008) 1031–1038.
- [20] S. Xu, Y. Wei, M. Kirkham, J. Liu, W. Mai, D. Davidovic, R.L. Snyder, Z.L. Wang, Patterned growth of vertically aligned ZnO nanowire arrays on inorganic substrates at low temperature without catalyst, *J. Am. Chem. Soc.* 130 (2008), 14958–.
- [21] S. Choi, Y. Zhou, W. Haske, J.W. Shim, C. Fuentes-Hernandez, B. Kippelen, ITO-free large-area flexible organic solar cells with an embedded metal grid, *Org. Electron.* 17 (2015) 349–354.
- [22] H.W. Choi, T. Zhou, M. Singh, G.E. Jabbour, Recent developments and directions in printed nanomaterials, *Nanoscale* 7 (2015) 3338–3355.
- [23] M. Singh, H.M. Haverinen, P. Dhagat, G.E. Jabbour, Inkjet printing-process and its applications, *Adv. Mater.* 22 (2010) 673–685.
- [24] T.B. Song, Y.S. Rim, F. Liu, B. Bob, S. Ye, Y.T. Hsieh, Y. Yang, Highly robust silver nanowire network for transparent electrode, *ACS Appl. Mater. Interfaces* 7 (2015) 24601–24607.
- [25] W. Tang, L. Feng, C. Jiang, G. Yao, J. Zhao, Q. Cui, X. Guo, Controlling the surface wettability of the polymer dielectric for improved resolution of inkjet-printed electrodes and patterned channel regions in low-voltage solution-processed organic thin film transistors, *J. Mater. Chem. C* 2 (2014) 5553.
- [26] D. Yang, Y.Q. Yang, Y. Duan, P. Chen, C.L. Zang, Y. Xie, D.M. Liu, X. Wang, Y.H. Duan, F.B. Sun, Q. Gao, K.W. Xue, Passivation properties of UV-curable polymer for organic light emitting diodes, *Ecs Solid State Lett.* 2 (2013) R31–R33.
- [27] D.J. Finn, M. Lotya, J.N. Coleman, Inkjet printing of silver nanowire networks, *ACS Appl. Mater. Interfaces* 7 (2015) 9254–9261.
- [28] J. Lee, I. Lee, T.S. Kim, J.Y. Lee, Efficient welding of silver nanowire networks without post-processing, *Small* 9 (2013) 2887–2894.
- [29] J. Chen, J. Liu, Y. Sakuraba, H. Sukegawa, S. Li, K. Hono, Realization of high quality epitaxial current-perpendicular-to-plane giant magnetoresistive pseudo spin-valves on Si(001) wafer using NiAl buffer layer, *Apl. Mater.* 4 (2016) 056104.
- [30] A.R. Madaria, A. Kumar, C.W. Zhou, Large scale, highly conductive and patterned transparent films of silver nanowires on arbitrary substrates and their application in touch screens, *Nanotechnology* 22 (2011).